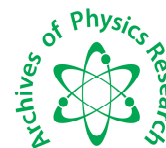




## Scholars Research Library

Archives of Physics Research, 2012, 3 (4):269-276  
(<http://scholarsresearchlibrary.com/archive.html>)



Scholars Research  
Library

ISSN : 0976-0970

CODEN (USA): APRRC7

### Photocatalytic degradation of Rose Bengal in visible light with Cr substituted $MnFe_2O_4$ ferrosipinel

P.P. Hankare<sup>a</sup>, A. V. Jadhav<sup>a\*</sup>, R.P. Patil<sup>a</sup>, K. M. Garadkar<sup>a</sup>, I. S. Mulla<sup>b</sup>, R. Sasikala<sup>c</sup>

<sup>a</sup>Department of Chemistry, Shivaji University, Kolhapur, India

<sup>b</sup>CSIR Emeritus Scientist, Centre for Materials for Electronics Technology, Pune 411008, India

<sup>c</sup>Chemistry Division, Bhabha Atomic Research Center, Mumbai 400085, India

#### ABSTRACT

In this work, we report synthesis of chromium substituted manganese ferrites nanoparticles by using sol-gel auto-combustion method. The phase formation of  $MnFe_{2-x}Cr_xO_4$  ( $0 \leq x \leq 2.0$ ) nanoparticles were identified by X-ray powder diffraction (XRD). Fourier transform infrared spectroscopy (FT-IR) and UV-VIS-NIR spectroscopy was used for photocatalytic study. The photocatalytic activity of the as-prepared ferrosipinels was evaluated by degradation of the flouorosein dye Rose Bengal under irradiation of visible light. The results showed that the increase in concentration of Cr in manganese ferrite increases photocatalytic activity efficiency towards degradation of Rose Bengal solution. This may be attributed to decrease in crystallite size with substitution of  $Fe^{+3}$  by  $Cr^{+3}$  ions.

**Keywords:** Ferrites, sol-gel auto-combustion method, visible light, Rose Bengal, photodegradation.

#### INTRODUCTION

Nowadays synthetic dyes have been commonly used in many industrial processes; especially in the textile industry, paper, printing and plastics industry. Synthetic dyes are classified according to their predominant chemical structures. The structural varieties of dyes include; acidic, reactive, basic, disperse, azo, diazo, anthraquinone-based, and metal complex. These dyes have very complex structures and low biodegradability. In addition, the highly complexed structured polymers of these dyestuffs cause substantial threat to the environment mainly due to their high stability and non-degradability and hence the decolorization/degradation of dye effluents has received a large attention [1-4].

In the last two decades various physical, chemical and biological pre-treatment and post-treatment techniques have been developed for the removal color from dye contaminated wastewater. Physical techniques like ion exchange method, adsorption on the activated carbon, coagulation by chemical agents, ultra filtration, reverse osmosis, use of ultrasonic radiations etc have been used. Along with this, various chemical methods like photosensitized oxidation, photocatalytic oxidation, adsorption, photo-Fentons method, and use of heterogeneous, homogenous catalysts were augmented in order to reduce the toxic effects of dye effluents [5-10].

The recent developments in water decontamination processes are concerned with the oxidation of these bio-recalcitrant organic compounds. These methods rely on the formation of highly reactive chemical species that

degrade more number of toxic compounds. Generally, anatase  $\text{TiO}_2$  is used for the photodegradation of different acidic, azo, diazo, anthraquinone-based dyes [11-13]. M. Lou et al [14] also used  $\text{TiO}_2$  deposited on black sand as a magnetic photocatalyst for removal of laboratory dyestuffs like Rose Bengal Rhodamine B. They observed that the photolysis of RB is not possible without using catalyst.

Photocatalytic bleaching of Rose Bengal by some colored semiconducting oxides were reported by Malkani et al. [15-16]. They reported effect of different semiconducting oxides such as  $\text{CuO}$ ,  $\text{NiO}$ ,  $\text{PbO}_2$  and  $\text{HgO}$  on photodegradation of Rose Bengal. The  $\text{PbO}_2$  shows better efficiency than  $\text{HgO}$  due to differences in band gaps of two semiconductor oxides. Similarly,  $\text{CuO}$  shows greater photoefficiency as compared to  $\text{NiO}$ .

Further, V. K. Sharma et al. [17] carried out photodegradation of Rose Bengal by using  $\text{MnO}_2$  as a photocatalyst. They reported spectrophotometric method for photocatalytic study. Wang et al. [18] reported photocatalytic degradation of Acid red 94 (Rose Bengal) using  $\text{TiO}_2$  membrane supported on a porous ceramic tube. The objective of this study was to find out the predominance of dead-end system. The effect of various parameters like initial dye concentration, catalyst loading, flow rate and light intensity was reported in this article.

Rose Bengal dye is extensively used in the printing, insecticides and in dyeing industries. However our literature survey does not reveal any result on the photocatalytic degradation of fluoroscein Rose Bengal dye by using nanosized ferrosinels. Hence we have taken up work on the photocatalytic degradation of Rose Bengal dye by using Cr doped manganese ferrite. In the present investigation, sol-gel auto combustion synthesized  $\text{MnFe}_{2-x}\text{Cr}_x\text{O}_4$  ( $0 \leq x \leq 2.0$ ) photocatalysts are utilized for photocatalytic degradation. The effect of various parameters such as pH of dye solution, initial concentration of dye solution, amount of catalyst used and adsorption studies were carried out.

## MATERIALS AND METHODS

### 2.1. Synthesis of catalyst

For synthesis of ferrosinels powder A. R. grade chemicals viz.  $\text{Mn}(\text{NO}_3)_2 \cdot 4\text{H}_2\text{O}$ ,  $\text{Fe}(\text{NO}_3)_3 \cdot 9\text{H}_2\text{O}$ ,  $\text{Cr}(\text{NO}_3)_3 \cdot 9\text{H}_2\text{O}$  and citric acid ( $\text{C}_6\text{H}_8\text{O}_7 \cdot 4\text{H}_2\text{O}$ ) were used. The metal nitrates solutions were mixed thoroughly in the required stoichiometric proportions in deionised distilled water. The pH value of the resultant solution was adjusted between 9.0 and 9.5 by drop-wise addition of dilute ammonia. The mixture was slowly heated ( $100^\circ\text{C}$ ) with constant stirring to obtain a fluffy mass. The precursor powder was sintered at  $1200^\circ\text{C}$  for 8h.

The rate of photocatalytic degradation of dyes and textile pollutants depends on several parameters such as pH, type of photocatalyst used, reactor configuration, dye concentration, amount of catalyst used and type of source used for the purpose of irradiation. Rose Bengal (Sodium salt of 4,5,6,7-tetrachloro-2',4',5',7'-tetraiodofluorescein) was used for degradation process. Its molecular structure is as shown in Fig 1.

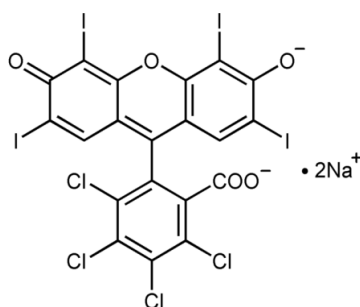


Fig.1. Molecular Structure of Rose Bengal

The photocatalytic degradation of Rose Bengal was studied in the presence of  $\text{MnFe}_{2-x}\text{Cr}_x\text{O}_4$  ( $0 \leq x \leq 2.0$ ) catalyst in visible light. 100ml of dye solution (50ppm) is taken in the test tube of photoreactor and irradiated with visible light (wavelength  $520 \pm 40$  nm), by adding 50 mg of catalyst for 5 h.

### 2.3. Instrumentation

The instruments used in this study were X-ray diffractometer, FT-IR spectrophotometer, UV-VIS-NIR spectrophotometer, photoreactor and pH meter. The X-ray diffraction patterns were recorded by an X-ray diffractometer (Model: Philips-PW-1710) using  $\text{CuK}\alpha$  radiation. The average crystallite size of prepared powders was calculated by using Scherrer relation from (311) peak values. The adsorption of study was carried out by using FT-IR spectrophotometer (Model: Shimadzu). Photocatalytic performance of the samples was determined by the UV-VIS-NIR spectrophotometer (Model: UV-3600). Photoreactor (Model: MLR-16) was used with lamp of wavelength  $520 \pm 40$  nm. The pH of samples was measured by pH meter (Model: Elico made). Microstructural analysis of the samples was carried out using a transmission electron microscope (TEM-Model: Philips 200 CX) operating at a voltage of 120 kV.

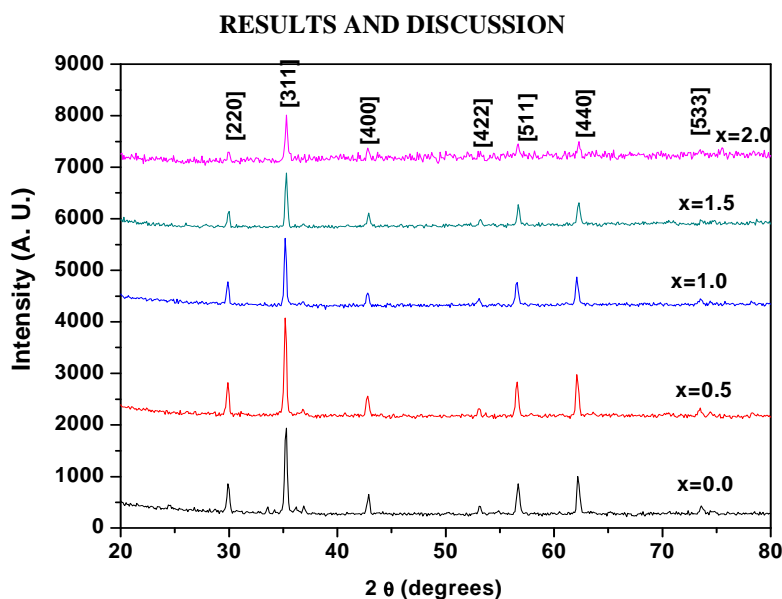


Fig.2. X-ray diffraction patterns of  $\text{MnFe}_{2-x}\text{Cr}_x\text{O}_4$  ( $0 \leq x \leq 2.0$ ) samples

Fig. 2 shows the XRD patterns of  $\text{MnFe}_{2-x}\text{Cr}_x\text{O}_4$  ( $0 \leq x \leq 2.0$ ) sintered ferrite powder. The XRD patterns clearly indicate that all these compositions have single phase cubic structure. All diffraction peaks match well with the normal characteristic diffraction pattern of  $\text{MnFe}_2\text{O}_4$  (JCPDF File no. 74-0419). The peaks can be indexed to planes (111), (220), (311), (222), (400), (422), (511) and (440) of pure spinel cubic structure. The crystallite size of sintered ferrite was calculated from the full width at half maxima (FWHM) of the most intense (311) peak by using Scherrer's formula. The various crystallographic parameters are summarized in Table 1.

Table 1. Crystallite size (D) and lattice constant of  $\text{MnFe}_{2-x}\text{Cr}_x\text{O}_4$  system.

Cr -content	Crystallite size in nm	Lattice constant (a) Å
0	55.98	8.453
0.5	54.87	8.452
1.0	53.81	8.451
1.5	52.14	8.433
2.0	51.72	8.430

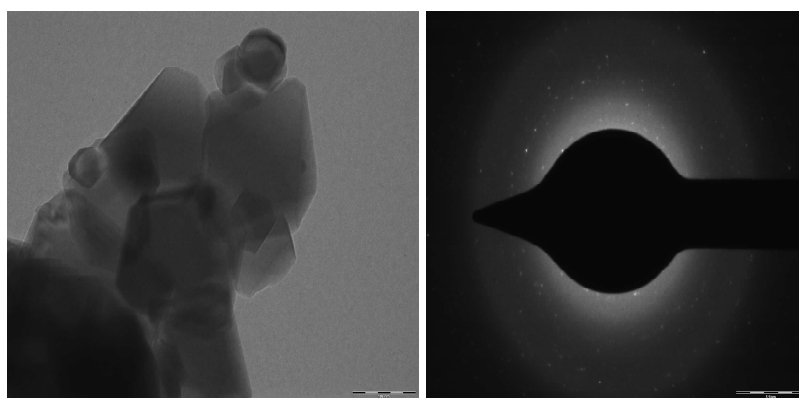
These values indicate a clear trend of decrease in the lattice constant with increasing chromium concentration. It can be attributed to the larger size of iron (ionic radii: 0.65 Å) than that of the chromium (ionic radii: 0.62 Å). It also supports the decrease in crystallite size with increase in chromium content. The theoretical and calculated values of Fe Mn and Cr contents are shown in Table 2.

Table.2. Elemental analysis with EDAX of the  $\text{MnCr}_x\text{Fe}_{2-x}\text{O}_4$  system

Composition (x)	Theoretical mass %			Observed mass % by EDAX		
	Mn	Fe	Cr	Mn	Fe	Cr
0	32.96	67.03	-	25.34	61.86	-
1	33.74	34.3	31.94	24.84	29.84	28.79
2	33.56	-	65.42	25.08	-	58.69

It is observed that theoretical composition of metals agrees quite well with the observed metal concentration.

Fig. 3a shows TEM image of  $\text{MnCr}_2\text{O}_4$ . The selected area electron diffraction pattern (SAED) for  $\text{MnCr}_2\text{O}_4$  is shown in Fig. 3b.

Fig.3. a) TEM image of  $\text{MnCr}_2\text{O}_4$  b) SAED pattern of  $\text{MnCr}_2\text{O}_4$ 

The SAED pattern showed intense ring pattern without any additional diffraction ring of secondary phase, revealing their single-phase spinel structure.

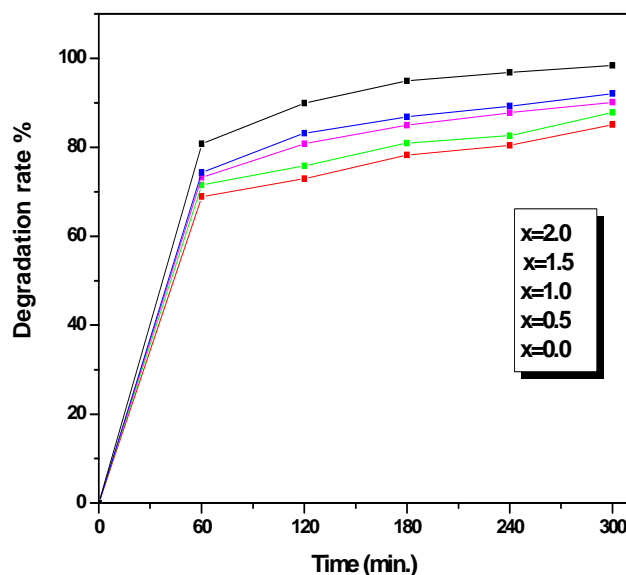
Fig.4. Photocatalytic degradation profiles of Rose Bengal over different irradiation time for  $\text{MnFe}_{2-x}\text{Cr}_x\text{O}_4$  ( $0 \leq x \leq 2.0$ ) samples

Fig. 4 shows photocatalytic degradation of Rose Bengal dye over different  $\text{MnFe}_{2-x}\text{Cr}_x\text{O}_4$  ( $0 \leq x \leq 2.0$ ) photocatalysts. Increase in the concentration of chromium in manganese ferrite provides greater efficiency for the photodegradation of Rose Bengal. The order of photocatalytic degradation of chromium doped  $\text{MnFe}_2\text{O}_4$  nanoparticles is as:  $\text{MnFe}_2\text{O}_4 < \text{MnFe}_{1.5}\text{Cr}_{0.5}\text{O}_4 < \text{MnFe}_{1.0}\text{Cr}_{1.0}\text{O}_4 < \text{MnFe}_{0.5}\text{Cr}_{1.5}\text{O}_4 < \text{MnCr}_2\text{O}_4$ . The  $\text{MnCr}_2\text{O}_4$  showing

maximum photocatalytic efficiency was used for further study on the effect of various parameters like pH, amount of catalyst used, concentration of dye solution and reusability.

Adsorption study was carried out by at different pH and the FTIR spectra obtained are shown in Fig 5 (a-e). From fig it is observed that adsorption of dye on the catalyst surface occurs mostly at pH 7. The spectrum of Rose Bengal shows carbonyl stretching ( $=C-O$ ) vibrations at  $1608\text{ cm}^{-1}$ .

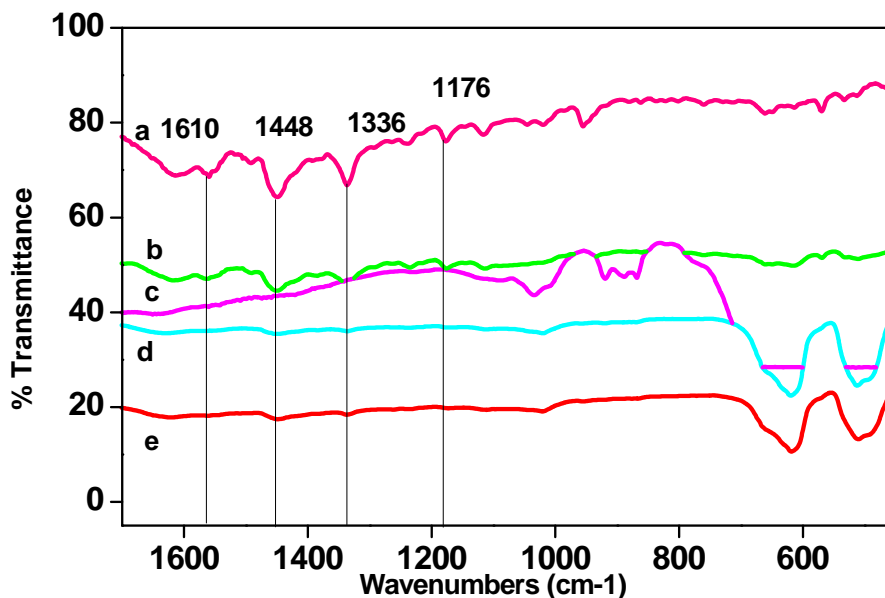


Fig.5. FT-IR spectra of a) Rose Bengal dye  $MnCr_2O_4$ , b) Rose Bengal dye adsorbed on  $MnCr_2O_4$  (pH=7), c)  $MnCr_2O_4$ , d) Rose Bengal dye adsorbed on  $MnCr_2O_4$  (pH=6), e) Rose Bengal dye adsorbed on  $MnCr_2O_4$  (pH=8)

This report is consistent with the previous reports [19-21]. The vibrations due to  $=C-H$  stretching were found at the  $2919$  and  $2848\text{ cm}^{-1}$  while the peaks due to  $C=C$  stretching were observed at  $1565$ ,  $1453$  and  $1332\text{ cm}^{-1}$ . These vibrations are also present in the RB (pH of dye solution =7) adsorbed on manganese chromite (Fig 5b) which confirms adsorption of dye on the surface of catalyst. The intensity of these two prominent peaks goes on decreasing with increase and decrease in pH of 7.

To study the effect of pH on photocatalytic degradation of Rose Bengal, a systematic study was carried out by variation of pH from 2-12 (Fig.6 a). It has been observed that pH plays an important role in the degradation of Rose Bengal dye. We observed a steady rise in the degradation up to 7 pH and then onward it decreases with increase in pH. Our observation matches well with the reported findings of Rauf *et al.* [22] wherein they too observed a similar pattern for the Rose Bengal dye decoloration on addition of  $H_2O_2$ . They attributed decoloration to the formation of  $OH^\bullet$  radicals on exposure to UV radiation. Xinyong Li *et al.* [23] in their studies on the Rhodamine B dye degradation reported formation of  $OH^\bullet$ ,  $HO_2^\bullet$ ,  $O_2^{\bullet-}$  in  $ZnFe_2O_4$ . The interaction between Rose Bengal dye molecule and the active catalytic surface of  $MnFe_{2-x}Cr_xO_4$  also plays a decisive role in the dye degradation.

The variation in concentration of dye also affects the photocatalytic activity. We varied the concentration of Rose Bengal from 10-400 ppm to find the effect on degradation. Fig. 6 (b) shows percent degradation at various dye concentrations. It was observed that the degradation rate gradually decreases with increase in the dye concentration. This may be due to increase in concentration of dye which prevents penetration of light to the surface of catalyst.

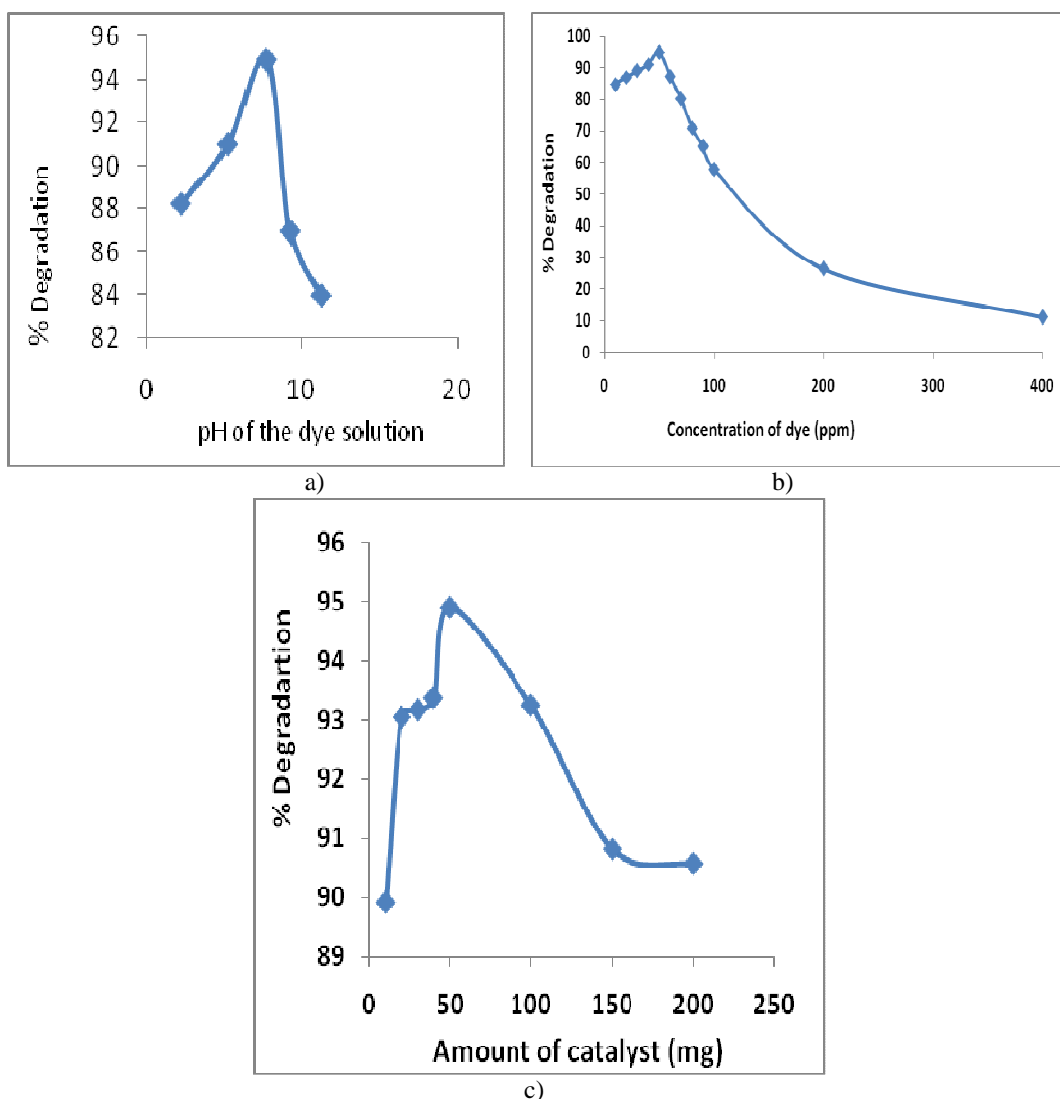


Fig.6. (a, b, c) Effect of decolouration of Rose Bengal (50ppm, irradiation Time: 5h) dye on variation of a) pH of dye solution, b) dye concentration, c) amount of catalyst

The variation in amount of catalyst also affects the rate of photodegradation. From Fig.6 (c) it is observed that the lower amount of catalyst is more suitable for photodegradation. As the amount of catalyst is increased the aggregation of particles leads to decrease in surface active sites. It may be considered like saturation point, above which any increase in the amount of catalyst has negligible or no effect on photodegradation of Rose Bengal. Increase in the amount of catalyst decreases the amount of light penetration through solution onto surface of catalyst.

The reusability of catalyst was studied by reactivating the used catalysts for four times. The catalyst is removed by filtration and activated at 100°C for 2 h and again used to study the reusability. Fig. 7 shows the reusability of the catalyst for four cycles. It has been observed that the percentage degradation decreases with further activation of the same catalysts. It may be due to fouling of catalyst and loss during filtration.

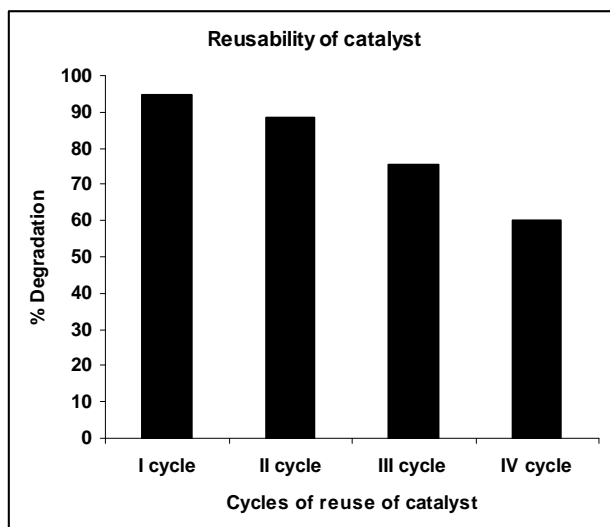


Fig.7. Reusability of catalyst for four times

### CONCLUSION

The photocatalytic degradation of Rose Bengal indicates that  $\text{MnFe}_{2-x}\text{Cr}_x\text{O}_4$  ( $0 \leq x \leq 2.0$ ) powders can effectively photodegrade Rose Bengal under visible light irradiation. The maximum photoactivity is achieved for  $\text{MnCr}_2\text{O}_4$ . The decrease in the concentration of the Rose Bengal dye is also due to the adsorption of dye particles on the surface of photocatalyst. Therefore,  $\text{MnCr}_2\text{O}_4$  can be used as potential photocatalyst for degradation of Rose Bengal in visible light.

### Acknowledgment:

Author (PPH) is thankful to DAE-BRNS, Mumbai for financial assistance through major research project.No.2009/37/41/BRNS/2231.

### REFERENCES

- [1] I. K. Konstantinou, T. A. Albanis, *Appl. Catal. B Environ.* **2004**, 49, 1-14.
- [2] A. Houas, H. Lachheb, M. Ksibi, E. Elaloui, C. Guillard, J. M. Hermann, *Appl. Catal. B Environ.*, **2001**, 31,145-157.
- [3] M. Dutta, J. K. Basu, M. H. Faraz, N. Gautam, A. Kumar, *Archives Appl. Sci. Res.*, **2012**, 4, 882-891.
- [4] H. Zhang, L. Duan, D. Zhang, *J. Hazard. Mater.*, **2006**, 138, 53-59.
- [5] W. S. Kuo, P.H. Ho, *Chemosphere*, **2001**, 45, 77-83.
- [6] X. Lv, Y. Xu, K. Lv, G. Zhang, *J. Photochem. Photobiol. A Chem.*, **2005**,173, 121-127.
- [7] C. Lopez, M. T. Moreira, G. Feijoo, J. M. Lema, *Biotechnol. Progress*, **2004**, 20, 74-81.
- [8] A. V. Salker, S. D. Gokakakar, *Int. J. Physic. Sci.*, **2009**, 4, 377-384.
- [9] R. Lall, R. Mutharasan, Y. T. Shah, P. Dhurjati, *Water Environ. Res.*, **2003**, 75, 171-179.
- [10] J. P. Lorimer, T. J. Mason, M. Plattes, S. S. Phull, D. J. Walton, *Pure Appl. Chem.*, **2001**, 73, 1957-1968.
- [11] C. A. Coutinho, V. K. Gupta, *J. Colloid Interface Sci.*, **2009**, 333,457-464.
- [12] M.A. Behnajady, N. Modirshahla, N. Daneshvar, M. Rabbani, *Chem. Eng. J.*, **2007**, 127, 167-176.
- [13] H. Zhang, D. Chen, X. Lv, Y. Wang, H. Chang and J. Li, *Environ. Sci. Tech.*, **2010**, 44, 1107-1111.
- [14] M. Luo, D. Bowden, P. Brimblecombe, *Water Air Soil Pollution*, **2009**, 198, 233-.
- [15] P. Ameta, A. Kumar, M. Paliwal, R. Ameta, R. K. Malkani, *Bull. Catal. Soc. India*, **2007**, 6, 130-135.
- [16] P. Ameta, A.Kumar, M. Paliwal, R. Ameta, R. K. Malkani, *Iran. J. Chem. Chem. Eng.*, **2010**, 29, 43-48.
- [17] N. Mittal, A. Shah, P. B. Punjabi, V. K. Sharma, *Rasayan J. Chem.*, **2009**, 2, 516-520.
- [18] W. Y. Wang, A. Irawan, Y. Ku, *Water Res.*, **2008**, 42, 4725-4732.
- [19] A. Uppal, B. Jain, P. K. Gupta, K. Das, *Photochem. Photobiol.*, **2011**, 87, 1146-1151.
- [20] Y. Guo, S. Rogelj, P. Zhang, *Nanotechnol.*, **2010**, 21,065102.
- [21] M. A. Jhonsi, A.Kathiravan, R. Renganathan, *J. Mol. Struct.*, **2009**, 921, 279-284.

- [22] M. A. Rauf, N. Marzouki, B. K. Korbahiti, *J. Hazard. Mate.*, **2008**, 159, 602-609.  
[23] X. Li, Y. Hou, Q. Zhao, L. Wang, *J. Colloid Interface Sci.*, **2011**, 358, 102-108.